FUTURE CHANGES IN BIOLOGICAL ACTIVITY IN THE NORTH PACIFIC DUE TO ANTHROPOGENIC FORCING OF THE PHYSICAL ENVIRONMENT

DAVID W. PIERCE

Scripps Institution of Oceanography, Climate Research Division, 0224, La Jolla, CA 92093-0224, U.S.A.
E-mail: dpierce@ucsd.edu

Abstract. Many studies have examined the physical changes expected in the environment as a result of anthropogenic forcing. These physical changes will have an effect on ecosystems as well. In this study, a nitrogen-phytoplankton-zooplankton (NPZ) model is used to examine the effects of changes in the physical environment on primary productivity in the North Pacific ocean. The physical variables considered are mixed layer temperature and depth, solar insolation, and large-scale upwelling. The changes in these fields by the 2090s are taken from a coupled ocean-atmosphere general circulation model forced by projected atmospheric CO_2 and sulfates, then applied to the NPZ biological model. The result is a change in the seasonal cycle of phytoplankton and herbivore concentrations across the subpolar North Pacific, moving from a regime characterized by strong variability with low wintertime values and a spring bloom, to much more constant yearly values. A reduction of yearly-averaged primary productivity accompanies much of this shift to more constant year-round conditions. In other regions, productivity increases as warmer surface waters enable higher growth rates. Changes in mixed layer temperature and depth account for almost all the changes in productivity; model-predicted changes in surface insolation and large-scale upwelling have little impact.

1. Introduction

Many studies have used coupled climate models to look at the physical changes expected in the world due to anthropogenic forcing. However, changes in the physical environment can have effects on ecosystems as well. Alterations in ecosystems, in turn, can have impacts on people and society; for example, fish populations affect both food supplies and jobs. Therefore, it is important to examine the predicted effects of changes in the environment on ocean ecosystems.

Ecosystems are too complicated to model in a complete way, so the following approach was adopted for this work. First, a few physical variables of interest that might change due to anthropogenic forcing were selected. Then, the simplest ecosystem model that depended on those variables of interest was chosen and this model's response to the environmental changes was analyzed. The understanding gained this way can form the basis for examining more complicated biological models in the future.

The physical variables of interest were the following:

Climatic Change **62:** 389–418, 2004.

1. Mixed layer depth. Deeper mixed layers can mix up more nutrients from below, but also are darker (less light-driven production) near the bottom.
2. Mixed layer temperature. Warmer temperatures allow higher growth rates.
3. Upwelling velocity. Large-scale changes in the surface wind field can affect how much nutrient-rich deep water is upwelled from below.
4. Solar insolation. The amount of sunlight falling on the ocean's surface might change due to changes in cloudiness or sea ice coverage. This will directly affect the phytoplankton's light-driven production.

Note that this study is focused specifically on how changes in the *physical* environment might modify ecosystems. Changes in the *biogeochemical* environment are interesting in their own right, and likely to be important, but not included in the work shown here. For example, increasing industrialization in eastern Asia is likely to result in enhanced iron or gaseous nitrogen deposition into the North Pacific in future years, which will have a separate effect on the biological activity. A review of such processes is given in Denman et al. (1996).

The predicted changes in physical variables were obtained from anthropogenically-forced runs generated by pilot accelerated climate prediction initiative (pilot-ACPI) program (Barnett et al., 2004). Although ACPI's focus was on hydrology in the western U.S., the global data set produced in that effort was appropriate for forcing a biological model. In the spirit of concentrating on ACPI's region of interest, attention will be focused on the North Pacific. Important fisheries are located in the North Pacific (e.g., salmon) that have a substantial effect on the economy of the western states. Polovina et al. (1995) have previously examined natural climate variability in this region using a biological model similar to that employed here.

Prior work in examining the effect of climate change on biological processes has often focused specifically on the 'biological pump', which are the set of processes involved in biological uptake of carbon in the mixed layer and the subsequent export of that carbon to the deep ocean. These processes are important because they help regulate atmospheric CO_2 concentrations; for example, models suggest atmospheric concentrations of CO_2 (which were $\sim$280 ppmv in pre-industrial conditions) would have been drawn down to $\sim$160 ppmv if the biological pump used all available surface nutrients, or would have risen to $\sim$450 ppmv in the total absence of marine production (Sarmiento and Toggweiler, 1984; Shaffer, 1993; Maier-Reimer et al., 1996; Sarmiento et al., 1998; see also the review in Denman et al., 1996). The work here differs in that it is not focused on the biological pump *per se*, so the feedback effects on atmospheric CO_2 concentrations are not considered. This is partly due to the technique used; the biological model is driven by a set of coupled climate model runs with specified atmospheric CO_2 conditions (Dai et al., 2004). The emphasis instead is on changes in the seasonal cycle of phytoplankton and herbivore populations in the North Pacific ocean. In this sense the work is more akin to that of Bopp et al. (2001), who used both a biogeochemical model

and a nitrogen-phytoplankton-zooplankton-detritus model to examine the effects of climate change. That study found a poleward shift of marine production, similar to that found here. The analysis in this work attempts to be more detailed, however; this is possible at least partly because of the focus on the North Pacific, while Bopp et al. modeled the entire globe.

The rest of this paper is organized as follows. In Section 2, the physical model used in the pilot-ACPI program is described. The biological model is described in Section 3 and the equations are given in Appendix A. Section 4 shows the changes in physical environment that the physical model projects for the decade of the 2090s. The biological model's response to these changes over the North Pacific is shown in Section 5. A more detailed analysis of the seasonal cycle at certain points of interest is given in Section 6. The discussion in Section 7 focuses on the key role of the effective growth rate in determining the biological model's response to the changing environment. Conclusions are given in Section 8.

2. Physical Model Overview

The physical model used here is the Parallel Climate Model (PCM), version 1 (Washington et al., 2000). Dai et al. (2004; in this issue) describe the model and simulations in detail, so only a brief outline will be given here.

The atmospheric component of the PCM is the CCM3 atmospheric general circulation model developed at the National Center for Atmospheric Research (Kiehl et al., 1998), a spectral model used at T42 resolution (equivalent to about 280 by 280 km grid spacing), and 18 layers in the vertical. CCM3 includes a land surface model that accounts for soil moisture and vegetation types, as well as a simplified runoff scheme.

The ocean component of PCM is the Parallel Ocean Program (POP), developed at the Los Alamos National Laboratory (Smith et al., 1992; Dukowicz and Smith, 1994), used at a horizontal resolution of 384 by 288 gridpoints (roughly 2/3° resolution), with 32 vertical levels. The vertical levels are clustered near the surface to improve resolution of the important surface mixing processes. A displaced-pole grid is used in the northern hemisphere to eliminate the problem of convergence of the meridians in the Arctic Ocean. It is worth noting that higher resolution runs of POP are an ongoing activity, for example, 0.28° resolution runs with an ecosystem model (Shaoping Chu, Los Alamos National Laboratory, personal communication). Since eddy pumping of nutrients is important to global biological activity, it will be interesting to compare future results that use truly eddy-resolving models to those shown here.

A dynamic-thermodynamic sea-ice model based on Zhang and Hibler (1997) is included, with an elastic-viscous-plastic rheology for computational efficiency (Hunke and Dukowicz, 1997). The ice model is formulated on its own grid, which has a total of 320 by 640 gridpoints, and a physical grid spacing of roughly 27 km.

The PCM runs start in 1870 and end in 2099, using historical estimates of atmospheric carbon dioxide and sulfates up until the present, and business-as-usual (BAU) projections of these quantities for future years. There are five ensemble members available for this work, but for these results only one ensemble member was used, as it represents expected future change to first order without leading to problems with interpreting averages in the presence of non-linearities (i.e., the response to averaged forcing is not the same as the averaged response to individual forcing for non-linear processes). The results shown here compare the decade of the 2000s to the decade of the 2090s.

3. Biological Model Overview

The biological model includes nitrogen, phytoplankton, and herbivores (a so-called NPZ model, with Z referring to herbivorous zooplankton), and is based on the work of Evans and Parslow (1985; EP85 hereafter). The equations for the model are given in Appendix A, while a schematic overview is shown in Figure 1. There is a well-mixed upper layer of thickness M and temperature T, both of which are specified from the physical model (PCM). The mixed layer contains phytoplankton, which are eaten by herbivores, which in turn are eaten by carnivores. The phytoplankton locally release nutrients back into the mixed layer via respiration. At the base of the mixed layer, both local turbulent exchange and large-scale upwelling mix nutrients up from below. The physical model does not incorporate a prognostic equation for nutrient concentrations, so they are specified at the base of the mixed layer from observations (Levitus, 1994).

The separation into the two mixing components (large-scale upwelling and local turbulent exchange) is a departure from the way vertical mixing was parameterized in EP85, which had only a fixed vertical exchange taking into account both these effects. Here, the large-scale upwelling is taken from the physical model, with a constant value used for the local turbulent exchange. Ideally, the local turbulent mixing would have been taken from the physical model as well; however, these terms were not saved in the physical model runs. Inclusion of the large-scale upwelling allows the biological model to adjust to large-scale changes in the wind field that drive different patterns of Ekman upwelling or downwelling. Upwelling carries more nutrients up into the mixed layer, while downwelling reduces the vertical flux of nutrients.

Solar forcing is taken from the physical model. This allows changes in the light-driven production if, for example, the physical model predicts systematic differences in cloudiness arising from anthropogenic forcing.

Following Sarmiento et al. (1993) and Polovina et al. (1995), the maximum growth rate is taken to be a function of mixed layer temperature as follows: $P_{\max} = 0.6(1.066)^T$, where T is the mixed layer temperature in °C.

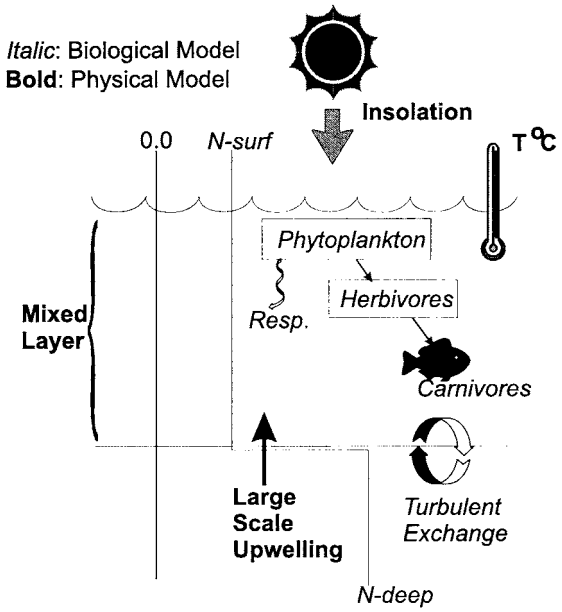

Figure 1. A schematic of the NPZ biological model. Forcing terms taken from the physical model are indicated in bold, while elements of the biological model are indicated in italic.

Biological model parameters are taken from EP85 with the few exceptions noted in Appendix A, and are appropriate to the extratropical region. Accordingly, we will focus on the area in the Pacific between 20° N and 70° N.

4. Physical Forcing

The changes in the four forcing variables (mixed layer temperature and depth, solar insolation, and upwelling velocity) will now be shown for the decade of the 2090s versus the 2000s, averaged both over the phytoplankton growing season March-April-May-June (MAMJ) and yearly.

4.1. MIXED LAYER TEMPERATURE

Figure 2 shows the changes in mixed layer temperature (decade of the 2090s minus 2000s). Temperatures are considerably warmer (by about 1.5–3.0 °C) during the 2090s; the warming is more pronounced in the more northerly part of the region. The temperature increase has only weak seasonality. Since the maximum growth rate depends monotonically on temperature, this warming means that growth rates in the 2090s will generally be higher than in the 2000s. PCM's climate sensitivity is about 1.5° C to a doubling of atmospheric CO_2 (Washington et al., 2000), which is on the low end of the frequently accepted range of 1.5 °C to 4.5 °C for various coupled climate models (IPCC, 2001).

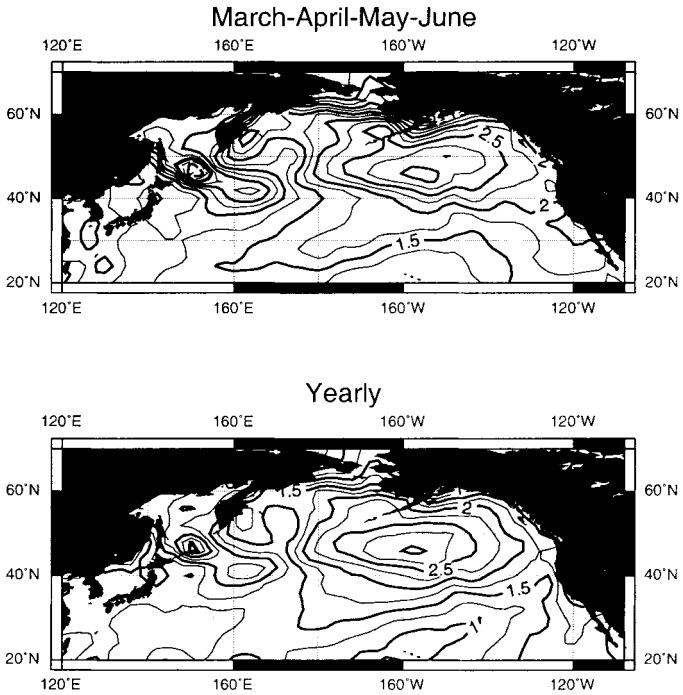

Figure 2. Difference in mixed layer temperature (C) between the decade of the 2090s and the decade of the 2000s. Top: averaged over the growing season (MAMJ). Bottom: averaged over the year. Contour interval is 0.25 °C.

4.2. SOLAR FORCING

Figure 3 shows the surface solar insolation in the physical model during the decade of the 2090s versus 2000s. There is a decrease in seasonal (highly reflective) sea ice in the far North Pacific that results in an increase in net surface solar insolation of about 10–15 W m^{-2}, primarily during the growing season (MAMJ). This increase in raw solar insolation is translated to an increase in photosynthetically active radiation (PAR) as in EP85.

4.3. UPWELLING VELOCITY

Figure 4 shows the large-scale upwelling calculated by the model. The sense of the vertical velocity is such that Ekman suction (upwelling) occurs over the subpolar gyre, while Ekman pumping (downwelling) is found over the subtropical gyre. Gargett (1977) has noted how the large scale features of the upwelling field shape the regional biological processes. Larger upwelling values can be seen along the coast (for example, the west coast of North America), which drives increased productivity in those regions. The difference between the vertical velocity in the 2000s and 2090s is small (Figure 4, bottom two panels), and it will be seen later that this change has little effect on the biology.

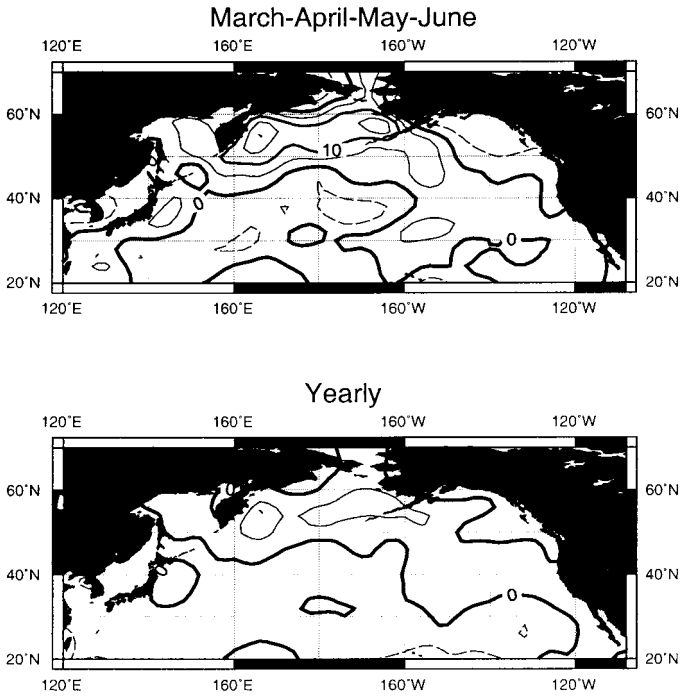

Figure 3. Difference in surface solar insolation (W m^{-2}) between the decade of the 2090s and the decade of the 2000s. Top: averaged over the growing season (MAMJ). Bottom: averaged over the year. Contour interval is 5 W m^{-2}. Negative contours are dashed.

4.4. MIXED LAYER DEPTH

Figure 5 shows the ratio of the mixed layer depth in the 2090s to the 2000s (the ratio is shown instead of the difference because of the large dynamic range). Over the majority of the Pacific north of 20° N, the ratio is less than one, indicating that mixed layer depths are thinner in the 2090s. The exception is a region near the Bering Sea, where depths are slightly greater in the 2090s. The depth of the mixed layer can have two contrasting effects on the biology; in light limited regions (generally the higher latitudes), a deeper mixed layer results in lower average illumination over the mixed layer depth, with a consequent decrease in phytoplankton growth rate averaged over the mixed layer. In nutrient limited regions (generally the lower latitudes), a deeper mixed layer increases the flux of nutrients from below, with an attendant increase in phytoplankton growth rates. Gargett (1997) described these competing effects in terms of an 'optimal stability window', in between the two extremes, where biological productivity is maximized.

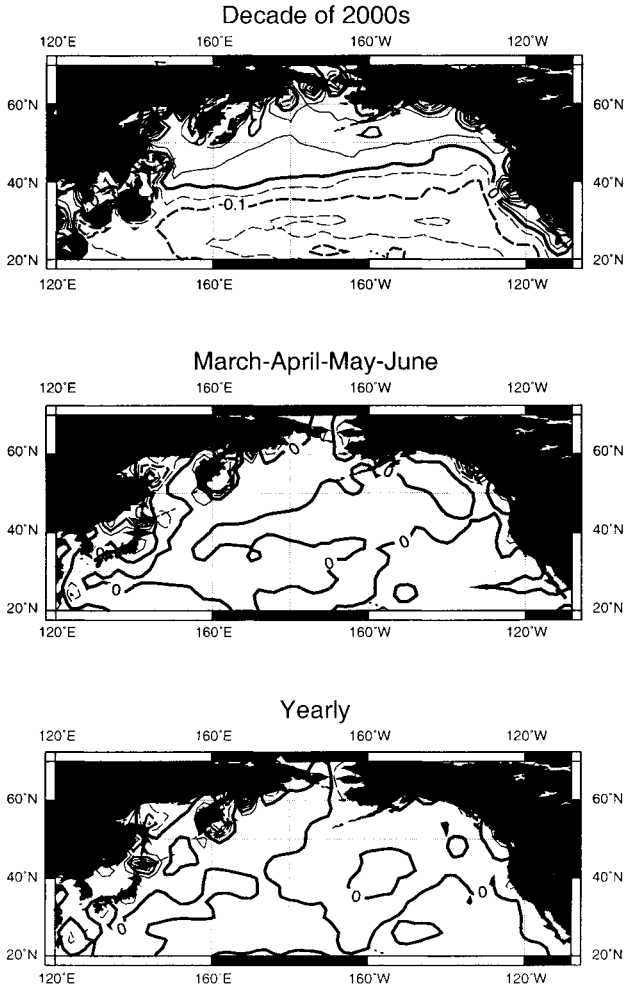

Figure 4. Upwelling velocity (m/day) at the base of the mixed layer. Top: for the decade of the 2000s. Middle: difference between decade of the 2090s and 2000s, averaged over the growing season (MAMJ). Bottom: difference averaged over the year. Contour interval is 0.05.

5. Biological Model Response

The response of the biological model to the environmental forcing outlined above will now be shown.

5.1. YEARLY CYCLE

The purpose of this work is to understand the reasons for changes in the ocean ecosystem between the 2000s and the 2090s, rather than to tune the model to

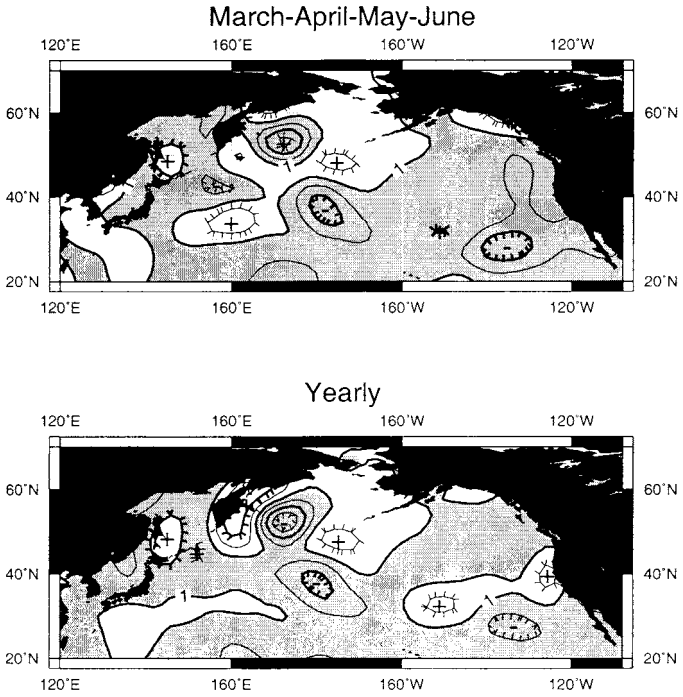

Figure 5. Ratio of the mixed layer depth in the 2090s to that in the 2000s. Top: averaged over the growing season (MAMJ). Bottom: averaged over the year. Contour interval is 0.05. Values less than 1 (indicating shallower mixed layers in the 2090s) are shaded.

reproduce current conditions as closely as possible. As such, no particular model parameter tuning for the purpose of matching observations was performed. Further, such tuning would have no effect on the conclusions presented in Section 8. Despite this, it still may be of interest to compare the seasonal dynamics of the NPZ model to observations in order to assess how close the model values are to reality. To do this, model fields will be compared to observed monthly SeaWiFS chlorophyll concentration data (obtained from http://daac.gsfc.nasa.gov/data /dataset /SEAWIFS /01_Data_Products /03_Gridded / 03_L3_Monthly_BRS/index.html) over the period 1998 to 2002.

The observed data cannot be straightforwardly compared to the model data because the former are pigment concentrations while the latter are nitrogen concentrations. However, for illustrative purposes, an approximate conversion is applied using a Redfield ratio of 106C:16N:1P, and assuming a constant carbon-to-chlorophyll a ratio of 50 mg carbon per mg chlorophyll a (geographical and temporal variability in the ratio is ignored; see, for example, Taylor et al., 1997).

Figure 6 shows the time evolution of zonally averaged phytoplankton concentration from the model compared to the (converted) observed values. In this figure the five years of observed data have been averaged into a climatology. Compared to

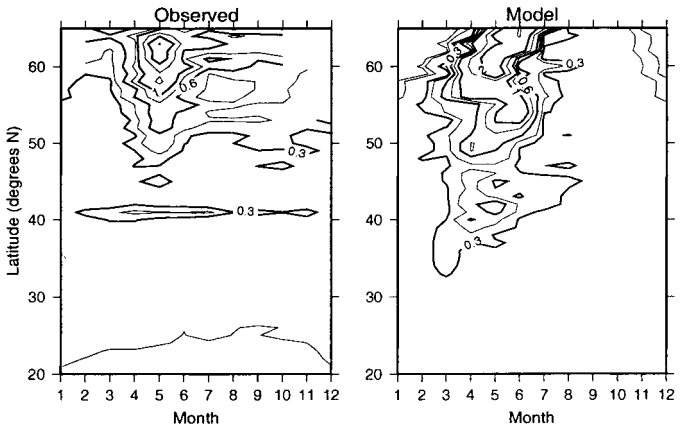

Figure 6. Time-latitude plot of zonally averaged phytoplankton concentration (mmN m^{-3}) estimated from SeaWiFS satellite observations (left) and from the NPZ model (right). Contours at 0.05, 0.1, 0.3, 0.4, 0.6, 0.8. 1.0, 1.5, 2.0, and 3.0.

the observations, the model starts the spring increase in phytoplankton concentration about a month earlier in midlatitudes, in March–April rather than April–May. There is also more tendency for the onset of growth to occur later at high northern latitudes in the model than in the observations. Both the model and observations show a tendency for the summer decay in high concentration values to happen later in the year at higher latitudes, however.

The model also has generally higher values than are seen in the observations. This is partially because the values evolved by the model are higher than observed, and partly because the bloom is more widespread in the model, resulting in larger zonal averages. This latter point is illustrated in Figure 7; shown are phytoplankton concentrations in May, at the peak of the spring bloom. The model generally shows a wider region with enhanced values. The notable exception to this is along the west coast of North America, where the model values are distinctly lower than observed. This is likely due to the biological model's use of a single, constant vertical turbulent mixing parameter (equivalent to 0.3 cm^2 s^{-1}; see Appendix A) that is appropriate to the open ocean. Enhanced mixing near the coasts, especially over the continental shelves, would tend to increase nutrient and phytoplankton concentrations in those regions, an effect that is currently ignored.

5.2. GROWING SEASON

Figure 8 shows the growing season phytoplankton concentration in the NPZ model, for the 2000s and 2090s. There is an arc of high values along the continental coasts, with generally higher values in the subpolar gyre (where the upwelling occurs) than in the subtropical gyre (downwelling). Values range from 0.27 mmN m^{-3} in the central subtropical gyre to greater than 2.0 mmN m^{-3} near the coasts.

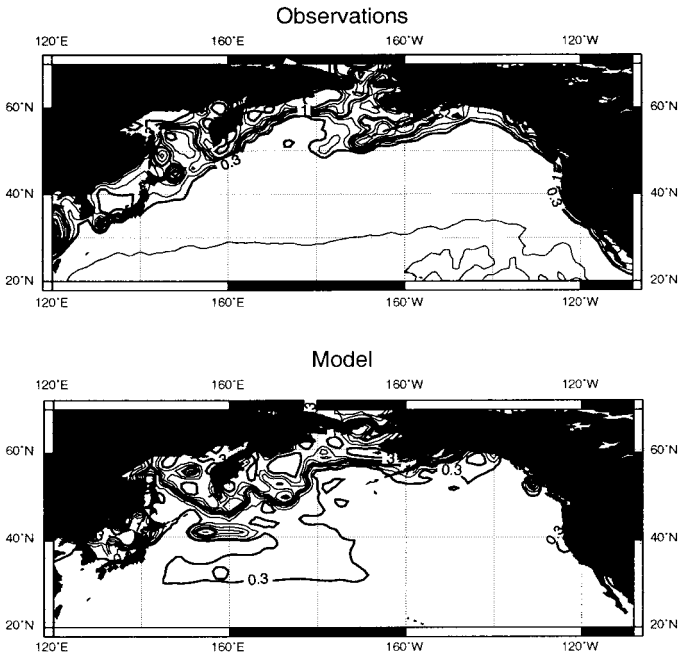

Figure 7. May phytoplankton concentrations (mmN m^{-3}) estimated from SeaWiFS satellite observations (top) and from the NPZ model (bottom). Contours as in Figure 6.

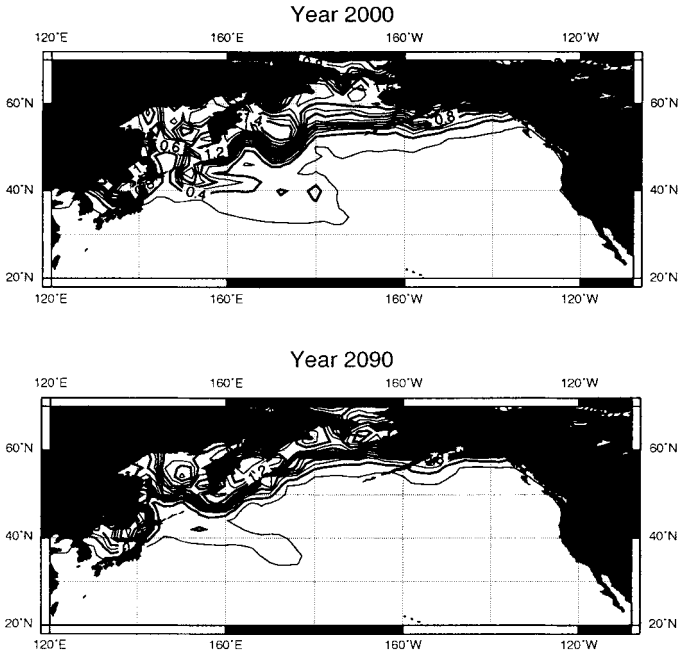

Figure 8. Growing season (MAMJ) phytoplankton concentrations (mmN m^{-3}) from the biological model. Top: decade of the 2000s. Bottom: the 2090s. Contour interval is 0.1.

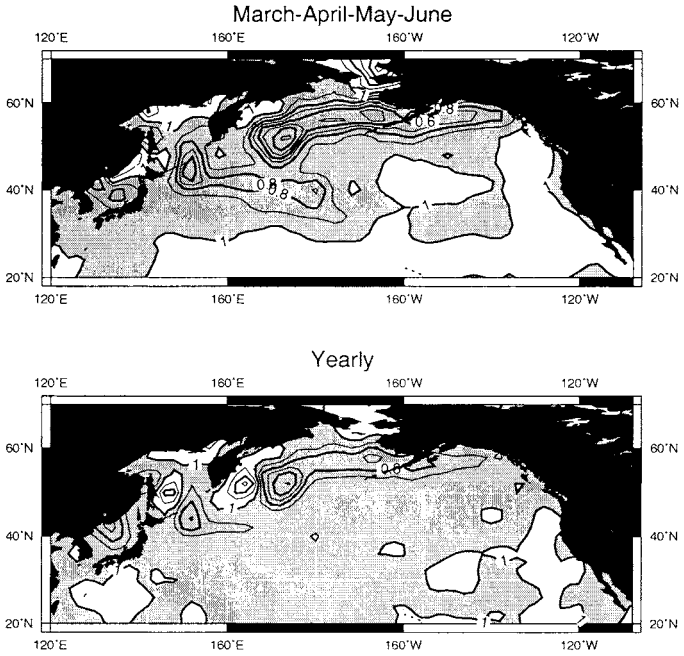

Figure 9. Ratio of phytoplankton concentration in the 2090s to the 2000s. Values less than one (indicating reduced concentrations in the later decade) are shaded. Top: averaged over the growing season (MAMJ). Bottom: averaged over the year. Contour interval is 0.1.

Figure 9 shows the ratio of phytoplankton concentration in the 2090s to the 2000s. Again, the ratio is used because of the large dynamic range involved. The main change is a decrease (ratio less than 1) in concentrations in the subpolar gyre; the reduction is on the order of 20–40% during the growing season, and 10–20% over the year. A predicted reduction in phytoplankton concentrations in the subpolar North Pacific is one of the primary results of the NPZ model; the reason for this decrease will be explained once all the changes in the biological model have been illustrated.

Figure 10 shows the ratio of the herbivores in the 2090s to that in the 2000s. The later decade has herbivore concentrations in the subpolar gyre that are 20–30% higher than in the earlier decade. This tendency can be understood from the equilibrium solutions (Appendix A; in particular, Equation (12)), where it is shown that the equilibrium herbivore concentration is directly proportional to the growth rate. (The equilibrium solutions are the phytoplankton, nitrogen, and herbivore concentrations that would be seen if the biological system responded instantaneously to the changing physical forcing. Departures from equilibrium conditions can lead to overgrazing and consequently low values of phytoplankton concentrations, or to unchecked population explosions that lead to spring blooms.)

The previous two illustrations were in terms of phytoplankton and herbivore concentrations. However, a more relevant quantity to the food chain is the primary

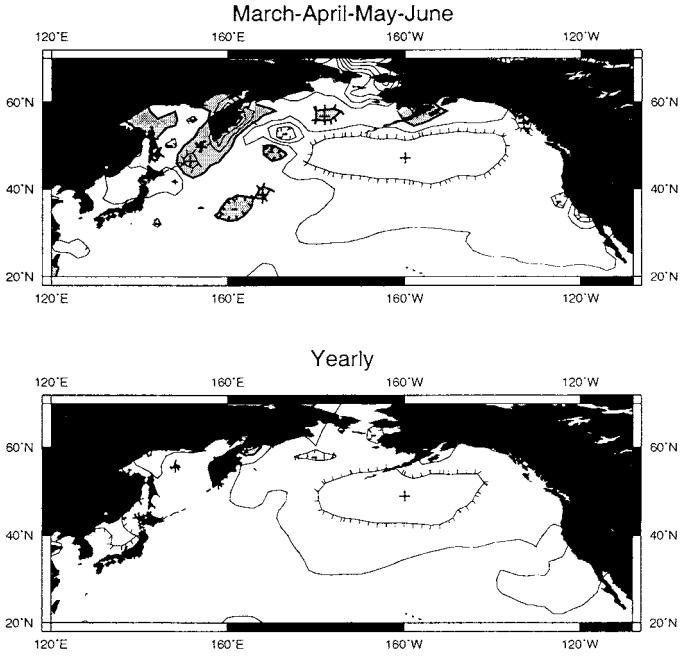

Figure 10. The ratio of herbivore concentration averaged over the decade of the 2090s over the decade of the 2000s. Values less than one (indicating reduced concentrations in the 2090s) are shaded. Top panel: averaged over the growing season (MAMJ). Bottom panel: averaged over the year. Contour interval is 0.1. Local maxima are indicated by '+' and local minima by '–'; ticks point in the downward direction.

productivity, R, defined as $R = PM\alpha$, where P is the phytoplankton concentration, M is the mixed layer depth, and α is the growth rate. The ratio of growth rates in the 2090s to the 2000s is shown in Figure 11. Growth rates are almost universally higher in the later decade. The increase in growth rate is driven primarily by the warmer mixed layer temperatures (Figure 2), since the maximum growth rate is taken to be a function of mixed layer temperatures. The effect of shallower mixed layers (Figure 5) can also be seen in those places where the shallowing is strong, and hence the mixed layer is better lit.

The ratio of primary productivity in the 2090s to the 2000s is shown in Figure 12 for both the growing season (top panel) and yearly averaged (bottom panel). During the growing season, the net result of the changes in phytoplankton concentrations, mixed layer depth, and growth rate is a reduction in productivity by 20–40% in the 2090s in the region of the subpolar gyre. In the Bering sea, by contrast, productivity increases by a similar amount. Averaged over the year, the reductions are smaller and in some places change sign. This is discussed in Section 7, but the gist is that there are two dynamic behaviors of the biological system. One is characterized by low wintertime concentrations of phytoplankton and herbivores, and high spring concentrations (spring blooms); the other, by much more even concentrations year-

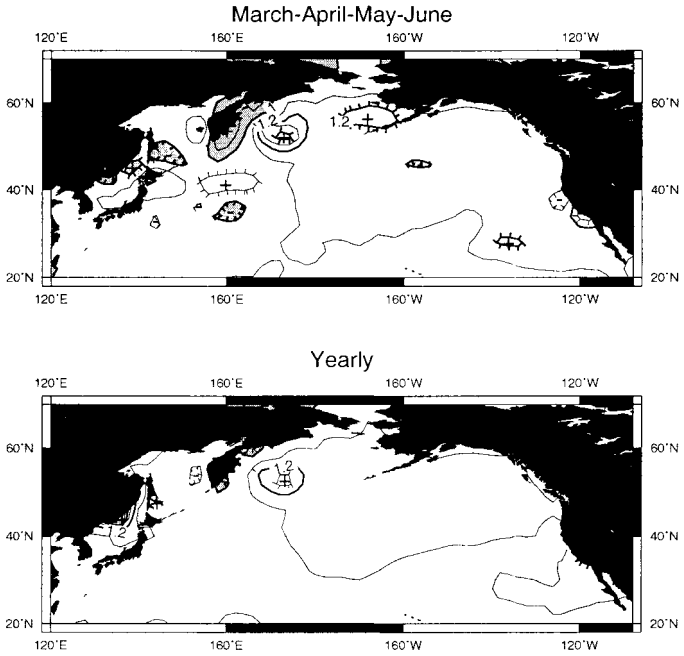

Figure 11. The ratio of growth rate in the 2090s over the 2000s. Values less than one (indicating lower growth rates in the 2090s) are shaded. Top panel: averaged over the growing season (MAMJ). Bottom panel: averaged over the year. Contour interval is 0.1. Local maxima are indicated by '+' and local minima by '–'; ticks point downgradient.

round. In places where spring blooms are lost (shaded regions in the top panel of Figure 12), the increase in productivity during the rest of the year partially makes up for the loss of the spring bloom, reducing the region of decreased productivity (lower panel of Figure 12).

6. Analysis

The biological model suggests that by 2090, phytoplankton concentrations and primary productivity will decrease in the subpolar North Pacific and increase in the subtropical Pacific and Bering strait. What physical forcings are responsible for the biological response in these regions, and why does the biological model respond with pronounced regional differences? The answers to these questions will allow an *understanding* of how the biology may respond to future environmental changes, rather than simply obtaining an *answer* from the biological model results. This allows evaluation of the model's response in a larger picture of uncertainty in predictions of future environmental changes.

In this analysis we will make use of the three points shown in the top panel of Figure 12: point A in the western North Pacific (170° E, 49° N); point B in the

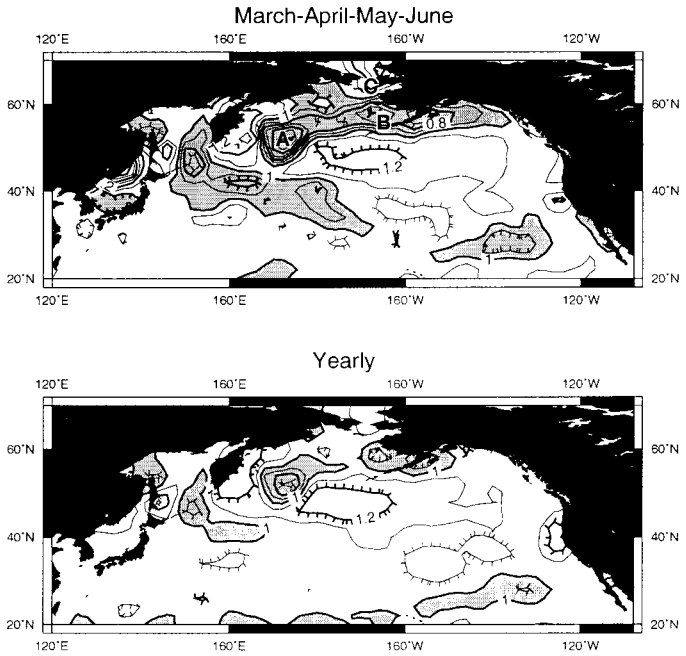

Figure 12. The ratio of primary productivity (mmN m^{-2} day^{-1}) for the decade of the 2090s over the decade of the 2000s. Values less than one (indicating reduced productivity in the latter period) are shaded. Top panel: averaged over the growing season (MAMJ). Bottom panel: averaged over the year. Contour interval is 0.1. Ticks point downgradient.

Aleutian Island region (165° W, 51° N); and point C in the Bering strait (167° W, 62° N). It should be understood that there is nothing special about these three particular points; they were selected because they exemplify the biological model's response in three dissimilar regions. Points were used, rather than averaging over regions of interest, because the non-linear nature of the biological model (Appendix A) means that the average biological response over a box is not the same as the response of the model to the average forcing over the box. Analysis at points avoids this problem, allowing a cleaner interpretation of the results. The understanding gained by examining these three points is broadly applicable over the entire domain; accordingly, these results will be extended to the entire North Pacific in Section 7.

6.1. WESTERN NORTH PACIFIC

The components of the physical forcing at point A, in the western North Pacific, are shown in Figure 13. The main difference between the 2000s and the 2090s is a strong reduction in winter mixed layer depth associated with the capping of the water column by the warmer water. Changes in upwelling and solar insolation are small by comparison.

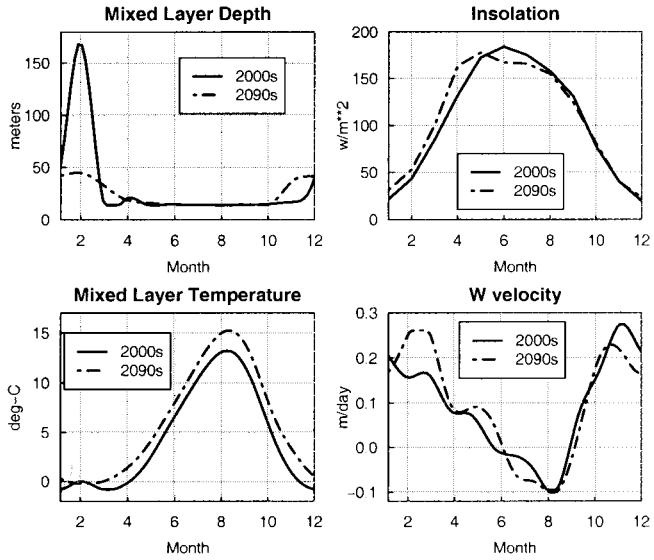

Figure 13. Components of the physical forcing for the decade of the 2000s (solid line) and 2090s (dashed line), at point A in the western North Pacific shown in Figure 12.

The biological model response at point A is shown in Figure 14. Concentrating for the moment on the contrast between the decade of the 2000s (thick solid line) and the 2090s (thick dashed line), it can be seen that the phytoplankton concentration (Figure 14a) undergoes a substantial yearly cycle in the 2000s, with low winter values and a strong spring bloom, but is nearly constant in the 2090s. This change is accompanied by an increase in herbivore concentration and *effective growth rate* (defined in Appendix A, Equation (6), this takes into account the phytoplankton growth rate, α, but is modified by losses due to respiration and vertical mixing).

To determine the physical forcings responsible for the biological response, four permutation test runs were performed. The standard run for the decade of the 2000s used the four forcing components (mixed layer temperature, mixed layer depth, large-scale upwelling, and solar insolation) from physical model with values averaged over the 2000s, and likewise for the 2090s run. For the permutation runs, *one* of the four forcing components was taken from the 2090s, while the rest were taken from the 2000s. This allows us to determine how the four forcings individually influence the changes in biology seen in the 2090s. (The final response will not be the sum of the four individual influences because of non-linearities.)

The results of the permutation runs at point A are also shown in Figure 14. For clarity, the annual cycles for the cases with permuted upwelling and solar forcing are omitted; it was found that changes in these forcings had little effect on the biological cycle. In panel 14a, comparing the results with only mixed layer temperatures taken from the 2090s (circles) to that with only mixed layer depths taken from the 2090s (squares), it can be seen that most of the change in phytoplankton

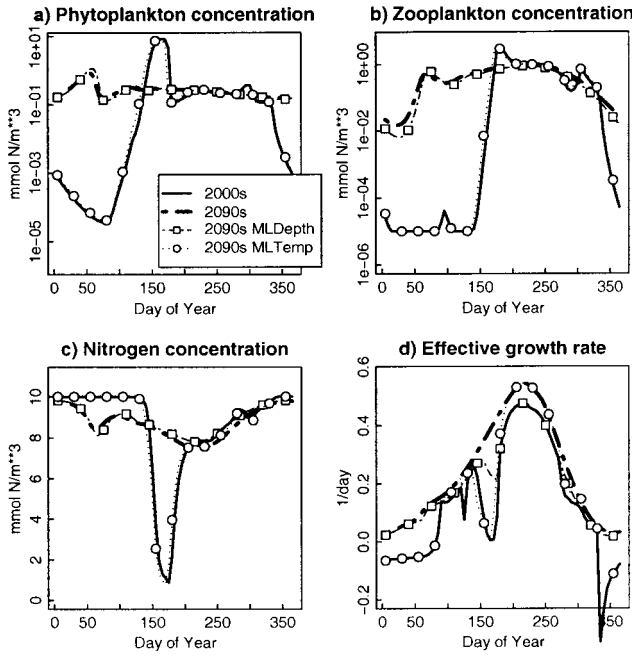

Figure 14. Annual cycle of phytoplankton, herbivore, and nitrogen concentrations (mmN m^{-3}), and effective growth rate (day^{-1}), from the biological model at point A in the western North Pacific. The physical forcing applied to the various runs is indicated in the legend.

and herbivore concentrations seen in the 2090s arise from changes in the mixed layer depth alone.

This can be understood from the results in EP85, which demonstrate that rapid specific changes in the growth rate enable the kind of spring bloom seen in the 2000s but not the 2090s. The effective growth rate, γ, is shown in Figure 14d. In this location, γ becomes negative in the dim midwinter months during the 2000s, as the phytoplankton concentration has negative tendencies due to respiration and the rapidly deepening mixed layer that exceed α. Phytoplankton concentrations drop, and with a smaller food source, zooplankton concentrations plummet. With the sudden shallowing of the mixed layer in the winter, γ becomes positive; the transition of γ through zero guarantees that the specific change in growth rate, $(1/\gamma)d\gamma/dt$, becomes large, leading inexorably to a spring bloom. This behavior does not occur in the 2090s, when the capping of the column by warmer surface water prevents γ from ever becoming negative (Figure 14d, squares). In other words, the phytoplankton in the 2090s are held closer to the surface in winter, where there is more light-driven production, and are not subject to dilution by a rapid increase in mixed layer depth. These effects keep the effective growth rate positive even in midwinter, maintain a more uniform year-round herbivore population. Along with the shallower mixed layer that reduces nutrient fluxes from below,

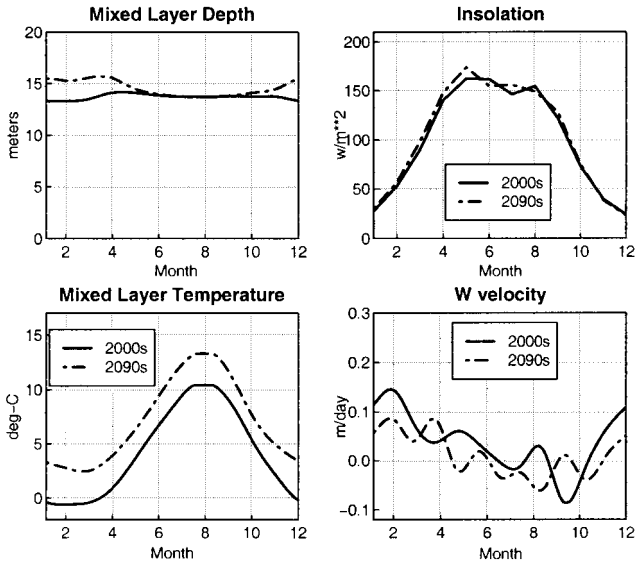

Figure 15. Components of the physical forcing for the decade of the 2000s (solid line) and 2090s (dashed line), at point B in the Aleutian Island region shown in Figure 12.

these changes prevent the specific growth rate from ever becoming large enough to trigger a spring bloom.

In summary, the biological model suggests that annual cycle of phytoplankton concentrations in the western North Pacific will change from one characterized by strong seasonal variation (with very low wintertime concentrations of phytoplankton and herbivores, followed by a spring bloom) to one characterized by much more uniform populations throughout the year. This happens because increasing stratification of the water column prevents a rapid late winter shallowing of the mixed layer, thereby eliminating the circumstances that formerly led to a spring bloom in the region.

6.2. ALEUTIAN ISLAND REGION

The components of the physical forcing at point B, in the Aleutian Island region, are shown in Figure 15. The region is characterized by a warming of mixed layer temperatures by almost 3 °C in the 2090s, along with modest changes in mixed layer depth and small changes in insolation and upwelling.

The biological response in the Aleutian Island region is shown in Figure 16. There is again a distinct reduction in the amplitude of the seasonal cycle of phytoplankton and herbivore concentrations in the 2090s. In this case, the permutation runs show that the change in mixed layer depth and temperature each separately have about the same effect, and it is the combination of the two that accomplishes the change in phytoplankton seasonal cycle.

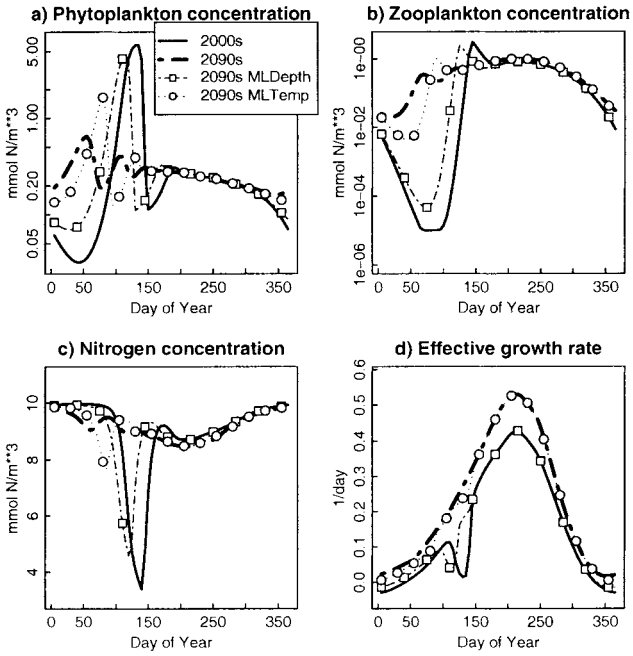

Figure 16. Annual cycle of phytoplankton, herbivore, and nitrogen concentrations (mmN m^{-3}), and effective growth rate (day^{-1}), from the biological model at point B in the Aleutian Island region. The physical forcing applied to the various runs is indicated in the legend.

The fact that warmer mixed layer temperatures reduce the peak phytoplankton concentration is, on the surface, somewhat counter-intuitive, since warmer mixed layer temperatures are associated with increases in the growth rate. This can again be understood by considering the effective growth rate (γ), Figure 16d. In the 2000s, γ becomes negative in midwinter (around day 345). As in the western North Pacific, γ increasing through zero leads inevitably to a spring bloom. However, the warmer surface temperatures and shallower mixed layer depths in the 2090s boost γ to the point where it never quite becomes negative (Figure 16d, thick dashed line). The size of the spring bloom is thus mitigated, and peak phytoplankton concentrations decrease.

The reason the temperature-driven increase in γ had little effect in the western North Pacific, while it is important here, is because γ contains contributions from both the mixed layer depth and temperature (Equation (6)). In the western North Pacific, the large changes in mixed layer depth overwhelm the changes due to temperature. In the Aleutian Island region, where the change in mixed layer temperature is about the same as in the western North Pacific but the changes in mixed layer depth are much more modest, both effects are important.

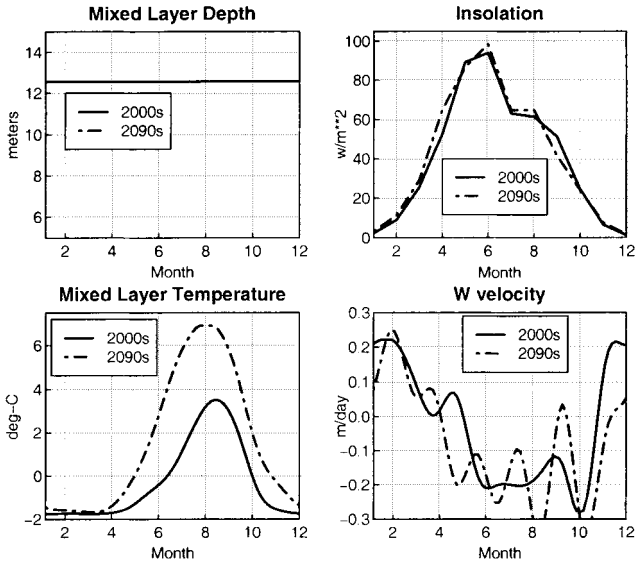

Figure 17. Components of the physical forcing for the decade of the 2000s (solid line) and 2090s (dashed line), at point C in the Bering strait shown in Figure 12.

6.3. BERING STRAIT

The components of the physical forcing at point C, in the Bering strait, are shown in Figure 17. The strong halocline in this region prevents any discernible change in mixed layer depth between the 2000s and 2090s. Insolation and vertical velocity changes are likewise small. The main difference in this region is an increase in mixed layer temperatures during the summer months, after the sea ice has retreated.

The biological response in the Bering strait is shown in Figure 18. The phytoplankton bloom comes slightly earlier in the year during the 2090s, a consequence of the earlier mixed layer warming. The overall amplitude and yearly evolution of the phytoplankton concentrations are otherwise similar between the two time periods. This is because the transition of γ through zero is almost the same in all cases (Figure 18d). This, in turn, is because the physical factors that affect γ are little changed between the two decades. In particular, the transition of γ through zero occurs early in the year, when the mixed layer temperature is the same. Consequently, the increase in productivity seen in the region (Figure 12) is due to summer increases in the growth rate (Figure 18d) forced by the warmer mixed layer temperatures, rather than by changes in phytoplankton concentration (as was found at points A and B).

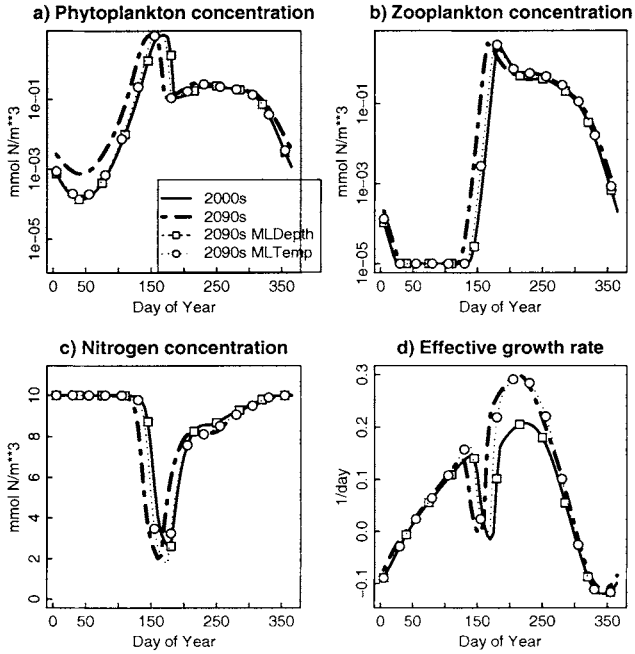

Figure 18. Annual cycle of phytoplankton (top) and herbivore (bottom) concentrations (mmN m^{-3}) from the biological model at point C in the Bering strait. The physical forcing applied to the various runs is indicated in the legend.

7. Discussion

The results in the previous section illustrate the importance of $\gamma_{\min}$, the yearly minimum value of the effective growth rate, in determining the seasonal cycle of phytoplankton and herbivore concentrations (c.f. Sverdrup's 1953 critical depth theory). Where $\gamma_{\min}$ drops below zero in midwinter, the subsequent transition of γ through zero in the spring leads to large values of the specific effective growth rate $(1/\gamma)d\gamma/dt$, and consequently to a spring bloom. Where $\gamma_{\min}$ never becomes negative, the specific effective growth rate generally stays large enough to prevent a bloom, and phytoplankton concentrations tend to be near their equilibrium values at all times. Physically, $\gamma_{\min}$ dropping below zero means that a deep mixed layer and weak sunlight (therefore low average illumination in the mixed layer) result in decreasing phytoplankton and (consequently) herbivore concentrations. The subsequent transition of $(1/\gamma)d\gamma/dt$ through zero in the spring, as the water column stratifies and insolation increases, implies that the herbivore population (whose growth lags that of the phytoplankton) cannot grow fast enough to keep up with the sudden explosive growth of the phytoplankton, and spring bloom results. More details are given in Appendix A.

This dependence on $\gamma_{\min}$ suggests partitioning the North Pacific into three regions based on the following criteria:

1. $\gamma_{\min} > 0$ in both the 2000s and 2090s. In these locations, phytoplankton and herbivore concentrations vary little over the year, and phytoplankton concentrations are not much different between the 2000s and 2090s. The main change in primary productivity in the 2090s therefore arises from changes in the phytoplankton growth rate α, which increases everywhere due to the mixed layer warming. In these regions modest increases in productivity are expected.
2. $\gamma_{\min} < 0$ in both the 2000s and 2090s. In these locations, the phytoplankton and herbivore concentrations undergo strong seasonal variability, with low wintertime values and strong spring blooms in both the 2000s and 2090s. In lieu of significant changes in the amplitude of the phytoplankton's seasonal cycle, future primary productivity is again most influenced by the effect of warmer surface waters on α. Therefore, primary productivity tends to increase in these regions.
3. $\gamma_{\min} < 0$ in the 2000s, but > 0 in the 2090s. In these regions, the physical forcings are such that a strong seasonal cycle in phytoplankton and herbivore populations (with low wintertime values and a subsequent spring bloom) is seen in the 2000s, but much more constant values are seen in the 2090s. The increase in $\gamma_{\min}$ in the 2090s can be accomplished by either greater stratification leading to decreased winter mixing (as seen at point A, in the western North Pacific; Section 6.1) or by warmer mixed layer temperatures acting together with modest changes in mixed layer depths (point B, in the Aleutian Island region; Section 6.2). In these locations, the more constant seasonal values result in decreased primary productivity in the spring, but greater productivity during the winter. The overall result is decreased productivity in most, but not all, regions where this happens (compare the bottom panel of Figure 12 to the top panel).

Figure 19 shows these three regions in the model. In the subtropics, $\gamma_{\min}$ is always positive (no shading), and there is little seasonal variability now or in the future. North of about 55° N, $\gamma_{\min}$ is always negative (stipple), and low wintertime phytoplankton concentrations with subsequent spring blooms are found. The main effect of anthropogenic forcing is to push the boundary of the region where strong seasonal variability is found farther to the north. This is because in the south, more constant daylight and warmer water temperatures keep the effective growth rate positive all year; in the north, the cold waters and weak sunlight in the winter enable the effective growth rate to drop below zero. There is necessarily a transition zone between the northern and southern regimes; and since the main effects of anthropogenic forcing relevant for the biology (warmer mixed layer temperatures and shallower mixed layer depths) both act in the direction of increasing $\gamma_{\min}$, the southern regime inevitably extends northwards. The simple biology of the NPZ model has a tendency to over-predict regions of strong seasonal variability, for example in the eastern North Pacific, where processes not considered here might come into play (e.g., iron limitation (Martin et al., 1990), changes in zooplankton

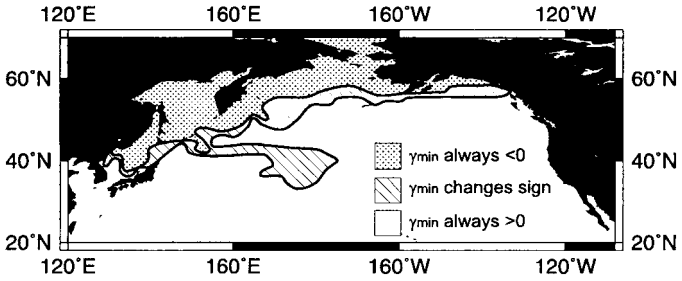

Figure 19. Regions where $\gamma_{\min}$ is negative in both the 2000s and 2090s (stipple), where $\gamma_{\min}$ is positive in both time periods (no shading); and where $\gamma_{\min}$ is negative in the 2000s but positive in the 2090s (crosshatch).

grazing (Frost, 1991), or deep mixing (Mitchell et al., 1991); see also Obata et al. (1996)). It may also be noted from the shaded regions of Figure 12, top panel, that the spring bloom goes away in a wider region than that given by the $\gamma_{\min}$ criterion (Figure 19). This is because $\gamma_{\min}$ dropping below zero is *sufficient* for a strong seasonal cycle with a spring bloom but not *necessary*; spring blooms can also result when $\gamma_{\min}$ gets very close to zero (but is still positive). The extra regions in Figure 12 where spring blooms are lost in the future are places where $\gamma_{\min}$ gets sufficiently close to zero to cause a spring bloom in the 2000s, but does not do so in the 2090s.

The conclusion that the region characterized by a strong seasonal cycle of phytoplankton and herbivore concentrations moves northward under anthropogenic warming is a robust prediction of the physical/biological model studied here. Different physical forcings (perhaps obtained from different coupled ocean-atmosphere models), or different parameters used in the biological model, will have the effect of shifting the particular latitudes where the regimes fall, but not in changing the behavior that anthropogenic forcing moves the spring bloom region northward. The only aspect of the physical forcing this conclusion depends on is that the warming signal in mixed layer temperature is monotonic over the region.

Regions that lose their ability to support strong seasonal cycles in phytoplankton concentrations tend to have less primary productivity when averaged over the year (although this is partly made up for by increased wintertime productivity). Elsewhere, the temperature-driven increase in growth rates will generally mean a higher primary productivity. In those regions that maintain their spring bloom (the far north), leading to large phytoplankton concentrations for a time, the absolute increase in primary productivity will be larger than in regions that are always near equilibrium phytoplankton concentrations (the region south of 50° N).

Although the results presented here are robust to details of the physical forcing, different biological systems than modeled here might behave differently. For example, in the real world, shifting distributions of species (each with their own way of reacting to the environment) might compensate for the changing environmental conditions. This question will need to be addressed by more elaborate biological

models. In such a case, the results from the simple NPZ model studied here should provide a framework for understanding the more complete (and, presumably, more complicated) results.

Comparing the results found here to previous work, Bopp et al. (2001) also found a poleward shift in marine productivity as a result of climate change. They attributed this to a longer growing season at the high latitudes, driven primarily by increased stratification leading to better photosynthetic efficiency in spring and summer. The similar results shown here could be seen as an examination of an analogous process from a different point of view. I.e., the analysis performed here in terms of $\gamma_{\min}$, as illustrated in Figure 19, provides a concise way of understanding the results that encapsulates the relevant biological and physical factors, as well as being a method for predicting how these results might apply to other regions. These results also have some similarities to the conceptual framework outlined in Gargett (1997), in that the regional changes in $\gamma_{\min}$, which are mainly effected by temperature-driven changes in water column stability, correspond to water columns moving into or out of 'optimal stability windows' for high biological productivity. However, this work shows that the view in terms of optimal stability windows is complicated by the time dependencies involved. Moving from a situation with low wintertime phytoplankton concentrations and a spring bloom to one with near-constant yearly values tends to result in a yearly averaged drop in productivity, since the spring bloom by itself generally accounts for a large fraction of the yearly averaged productivity. It does not guarantee a drop, however, since productivity during the winter increases.

8. Conclusions

Anthropogenic forcing can be expected to have an effect on ecosystems that respond to changes in the physical environment. One example is the ocean ecosystem, where phytoplankton concentrations depend on water temperature, sunlight, mixed layer depth, and the upwelling of nutrients from below. This study has used the environmental predictions of a coupled ocean-atmosphere general circulation model run to the 2090s to force a NPZ (nitrogen-phytoplankton-zooplankton) biological model of the North Pacific. The physical variables considered were mixed layer temperature, mixed layer depth, surface solar insolation, and large-scale upwelling and downwelling.

It was found that there is a northward shift of the region that shows large seasonal cycles in phytoplankton and herbivore concentrations, roughly between 150° E and 140° W, 50° N and 60° N. This is accompanied by a decrease in springtime primary productivity, which is partially counteracted by an increase in wintertime productivity. Productivity increases year-round in the Bering straits and subtropical Pacific, driven mostly by warmer water temperatures increasing the growth rate.

This behavior can be understood by considering the phytoplankton's effective growth rate γ, which is the growth rate modified to take into account losses due to respiration and vertical mixing. North of about 50° N, γ becomes negative in the dim midwinter months; in the south, it is always positive. Large changes in the specific effective growth rate $(1/\gamma)d\gamma/dt$ lead to spring blooms, so in places with negative midwinter values of γ, spring blooms occur after γ transitions through zero. The primary effects of the anthropogenic forcing are to warm the mixed layer and (more regionally) to increase stratification, decreasing mixed layer depths. Both tend to increase midwinter values of γ, in some places going from negative values in midwinter to positive values. This moves the region characterized by a strong seasonal cycle in phytoplankton concentrations, with low wintertime values and a spring bloom, farther to the north. The loss of spring blooms in the area left behind leads to lower springtime primary productivity in that region, and, to a lesser extent, lower productivity when averaged over a year. In regions where the seasonal cycle of phytoplankton concentrations does not change in the 2090s, productivity increases due to the higher growth rate (which itself arises from the warmer waters).

The main conclusion of this work – that the region of low winter phytoplankton concentrations and subsequent spring blooms moves northwards due to anthropogenic forcing, leaving behind a region with more constant yearly values – is robust to details of the physical forcing used. Environmental changes from a different coupled ocean-atmosphere model would likely have given a similar result (although the exact latitude of the regions might well be different) as long as the mixed layer warming is monotonic over the region. Changing the parameters for the biological model would similarly not change this conclusion, but rather would influence the exact latitudes involved. It should be kept in mind, however, that this conclusion might be modified by taking into account biological processes neglected in the simple NPZ model. For instance, were other species with different metabolic attributes or sensitivities to the environment included, the biology might respond by shifting the proportion of species instead. Or, an increase in abundance of nitrogen fixing phytoplankton, perhaps in response to the increasing vertical stratification, would have an impact on the seasonal cycle that is not included here. Consideration of such issues awaits results from more complex biological models.

Finally, note that this study attempts to isolate the effects of changes in the *physical* environment (mixed layer temperature and depth, upwelling, and solar insolation). Changes in the *biogeochemical* environment will likely have an influence as well (for example, increased iron deposition from enhanced industrialization in East Asia). These additional influences on the biology of the North Pacific await further study.

Acknowledgments

The author would like to thank Douglas Nielson and Tim Barnett of SIO for helpful discussions. This work was supported by the Department of Energy under grant DE-FG03–98ER62505. The computations for the pilot-ACPI project were carried out under the auspices of the National Partnership for Advanced Computer Infrastructure (NPACI) at the San Diego Supercomputer center, with the help of Peter Arzberger and Giridhar Chukkpalli. Additional runs were done at the Oak Ridge National Laboratory, with the help of John Drake, and we acknowledge the Center for Computational Sciences-Climate and Carbon Research (CCS-CCR) at Oak Ridge for computational resources used in support of this project. The comments of anonymous reviewers helped improve the manuscript, and are gratefully acknowledged.

Appendix A: Biological Model Equations

The biological model used here is similar to that described in EP85, with only a minor difference due to the splitting of the vertical mixing term into two components, large-scale upwelling and local turbulent mixing. The equations will be shown here for completeness and because the equilibrium model equations (also derived below) are based on the entire biological model, rather than on a reduced form of the model as was done in EP85. The model is formulated in terms of the mixed layer depth, M, dissolved nitrogen concentration, N, and the concentration of nitrogen held in the phytoplankton (P) and herbivores (H). The time evolution of these quantities is given by:

$$\dot{M} = \zeta(t) \tag{1}$$

$$\dot{N} = -\gamma P + \mu(N_o - N - P) \tag{2}$$

$$\dot{P} = \gamma P - zH \tag{3}$$

$$\dot{H} = \left(fz - g - \frac{\zeta(t)}{M} \right) H \,. \tag{4}$$

The rate of mixed layer deepening, $\zeta(t)$, is taken from the physical model. The vertical mixing term, μ, is given by:

$$\mu = \frac{m_e + m_t + \zeta^+(t)}{M} \,, \tag{5}$$

where m_e is the large-scale upwelling or downwelling driven by Ekman processes (values taken from the physical model), m_t is a local turbulent exchange at the base of the mixed layer, and $\zeta^+(t) = \max(\zeta(t), 0)$ is the entrainment rate. The vertical

mixing term in the herbivore equation is unlike that in the other equations (using ζ instead of ζ^+) because herbivores are assumed able to move up in the water column during times of detrainment.

The *effective growth rate* term, γ, is given by:

$$\gamma = \frac{\alpha(t, M, P)N}{j + N} - r - \mu \,. \tag{6}$$

It takes into account the phytoplankton growth rate, α, as well as losses to respiration (r) and vertical mixing (μ). Because γ is the dynamically important variable, not α, most of our analysis is done in terms of γ.

The term describing grazing of phytoplankton by herbivores, z, is given by:

$$z = \frac{c(P - P_0)}{K + P - P_0} \,. \tag{7}$$

The meaning and values taken for the other parameters is the same as in EP85 (their Table 1), and so are not repeated here, with the following exceptions. The local turbulent exchange, m_t, is taken to be 0.88 m day^{-1} ; this value is equivalent to the amount exchanged in one day at the base of a vertical distribution with an initial step-function, given a large-scale vertical diffusivity of 0.3 cm^2 sec^{-1}. The attenuation of light due to water is taken to be 0.04, and the attenuation due to self-shading by the phytoplankton is taken to be 0.06; these values are taken from the subarctic Pacific experiment of EP85.

8.1. A.1. EQUILIBRIUM SOLUTIONS

The equilibrium solutions to the model equations are obtained by setting the time derivatives to zero. The equilibrium phytoplankton concentration is:

$$P^* = P_0 + \frac{K}{\phi - 1} \,, \tag{8}$$

where $\phi = fc/(g - \zeta/M)$ represents a net grazing efficiency of the phytoplankton by the herbivores, and is the ratio of the nitrogen input to the herbivores by grazing to the nitrogen lost from the herbivores to carnivores or vertical mixing. For the values used here, $\phi \sim 7$. Thus, roughly speaking, $P^* \sim P_0 + K/6 \sim 0.27$. This is a direct function of the grazing threshold P_0, and modified by a term inversely proportional to the net grazing efficiency. If the herbivore's grazing efficiency (f) or rate (c) decreases, ϕ decreases and there are more phytoplankton in equilibrium (P^* increases). If the loss of herbivores to carnivores (g) increases, then ϕ decreases and again the equilibrium phytoplankton concentration increases.

The equilibrium nitrogen concentration is the solution to a quadratic equation, $(-b + (b^2 - 4ac)^{1/2})/2a$, where

$$a = 1 \tag{9}$$

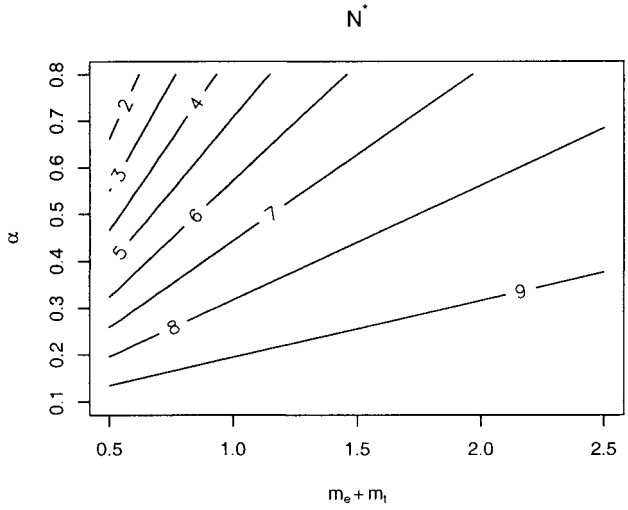

Figure 20. Equilibrium nitrogen concentration (mmN m^{-3}) as a function of total vertical mixing ($m_e + m_t$; m day^{-1}) and growth rate (α; day^{-1}).

$$b = \frac{(\alpha - r)P^*}{\mu} + j - N_0 \tag{10}$$

$$c = -j\left(\frac{rP^*}{\mu} + N_0\right). \tag{11}$$

Although the solution to this is algebraically complicated, over a reasonable range of parameters the strongest dependence is on α, N_0, and the vertical mixing ($m_e + m_t$). The dependence on N_0 is straightforward and unsurprising; the greater the deep nitrogen concentrations, the greater the equilibrium value in the mixed layer is. The dependence on ($m_e + m_t$) and α is shown in Figure 20, with all other values at their defaults for the biological model and a mixed layer depth of 30 m. At larger mixing rates concentrations approach the deep value ($N_0 = 10$); as the vertical mixing decreases, the growth rate has a stronger effect on the equilibrium nitrogen concentration, with larger growth rates leading to lower nitrogen levels.

The equilibrium herbivore concentration is:

$$H^* = \phi P^* \gamma / c\,. \tag{12}$$

Thus, the equilibrium herbivore concentration increases when their food source (P^*) or net grazing efficiency (ϕ) increases, and is proportional to the effective growth rate (γ). Note in particular that the equilibrium phytoplankton concentration is not dependent on the effective growth rate, while the equilibrium herbivore concentration is. In other words, increases in the growth rate translate to a larger herbivore population needed to eat the increased growth, while the phytoplankton population itself depends only on the efficiency of that grazing.

As outlined in EP85, disequilibrium conditions (and typically, a spring bloom) result when the specific rate of change of the equilibrium herbivore concentration, $(1/H^*)dH^*/dt$, is changing too rapidly to be tracked by the actual herbivore concentrations $(1/H)dH/dt$ (there is no issue with P^* changing too rapidly to be tracked since it is constant). From Equation (12),

$$\frac{1}{H^*}\frac{dH^*}{dt} = \frac{1}{\gamma}\frac{d\gamma}{dt}\,. \tag{13}$$

In particular, if γ increases through zero, the herbivore population is incapable of adjusting quickly enough to the altering environment, and a spring bloom generally results as the phytoplankton growth is unchecked by a sufficient herbivore population.

It is worth specifically pointing out the physical picture corresponding to disequilibrium conditions and spring blooms (cf. Sverdrup, 1953; Evans and Parslow, 1985). In locations where the mixed layer deepens dramatically in winter, average light levels in the mixed layer drop to low values, leading to drops in the phytoplankton concentration. At this time γ can become small or even negative. As a consequence of the diminished food supply, the herbivore population drops to a low level as well. In spring, the water column can stratify quickly and the insolation increase dramatically. γ becomes positive, and the transition of γ through zero means that the specific rate of change, $(1/\gamma)d\gamma/dt$ becomes infinite. In this disequilibrium condition the reduced herbivore population is lagging behind the exploding phytoplankton population, and the herbivores are unable to graze rapidly enough and reproduce quickly enough to prevent a period of runaway growth by the phytoplankton. The resulting spring bloom is eventually brought under control by nutrient depletion and growth of the herbivore population, and subsequently the phytoplankton and herbivore populations relax back towards equilibrium values.

References

Barnett, T. P., Malone, R., Pennell, W., Stammer, D., Semtner, A., and Washington, W.: 2004, 'The Effects of Climate Change on Water Resources in the West: Introduction and Overview', *Clim. Change* **62**, 1–11.

Bopp, L., Monfray, P., Aumont, O., Dufrense, J.-L., Le Treut, H., Madec, G., Terray, L., and Orr, J. C.: 2001, 'Potential Impact of Climate Change on Marine Export Production', *Global Biogeochem. Cycles* **15**, 81–99.

Dai, A., Washington, W., Meehl, G., Bettge, T., and Strand, G.: 2004, 'The ACPI Climate Change Simulations', *Clim. Change* **62**, 29–43.

Denman, K., Hofmann, E., and Marchant, H.: 1996, 'Marine Biotic Responses to Environmental Change and Feedbacks to Climate', in Houghton, J. T., Filho, L. G. M., Callander, B. A., Harris, N., Kattenberg, A., and Maskell, K. (eds.), *Climate Change 1995*, Cambridge University Press, New York, pp. 485–516.

Dukowicz, J. K. and Smith, R. D.: 1994, 'Implicit Free-Surface Method for the Bryan-Cox-Semtner Ocean Model', *J. Geophys. Res.* **99**, 7991–8014.

Evans, G. T. and Parslow, J. S.: 1985, 'A Model of Annual Plankton Cycles', *Biological Oceanography* **3**, 327–347.

Frost, B. W.: 1991, 'The Role of Grazing in Nutrient-Rich Areas of the Open Sea', *Limnol. Oceanogr.* **36**, 1616–1630.

Gargett, A. E.: 1997, 'Physics to Fish: Interactions between Physics and Biology on a Variety of Scales', *Oceanography* **10**, 128–131.

Hunke, E. C. and Dukowicz, J. K.: 1997, 'An Elastic-Viscous-Plastic Model for Sea Ice Dynamics', *J. Phys. Oceanog.* **27**, 1849–1867.

IPCC: 2001, *Climate Change 2001: Synthesis Report*, Contribution of Working Groups I, II, and III to the Third Assessment Report of the Intergovernmental Panel on Climate Change, Cambridge University Press, 397 pp.

Kiehl, J. T., Hack, J. J., Bonan, G. B., Boville, B. A., Williamson, D. J., and Rasch, P. J.: 1998, 'The National Center for Atmospheric Research Community Climate Model: CCM3', *J. Climate* **11**, 1131–1149.

Levitus, S.: 1994, *World Ocean Atlas 1994*, U.S. Dept. of Commerce, National Oceanic and Atmospheric Administration, 552 pp.

Maier-Reimer, E., Mikolajewicz, U., and Winguth, A.: 1996, 'Future Ocean Update of CO_2: Interaction between Ocean Circulation and Biology', *Clim. Dyn.* **12**, 711–721.

Martin, J. H., Gordon, R. M., and Fitzwater, S. E.: 1990, 'Iron in Antarctic Waters', *Nature* **345**, 156–158.

Mitchell, B. G., Brody, E. A., Holm-Hansen, O., McClain, C., and Bishop, J.: 1991, 'Light Limitation of Phytoplankton Biomass and Macronutrient Utilization in the Southern Ocean', *Limnol. Oceanogr.* **36**, 1662–1677.

Obata, A., Ishizaka, J., and Endoh, M.: 1996, 'Global Verification of Critical Depth Theory for Phytoplankton Bloom with Climatological *in situ* Temperature and Satellite Ocean Color Data', *J. Geophys. Res.* **101**, 20657–20667.

Polovina, J. J., Mitchum, G. T., and Evans, G. T.: 1995, 'Decadal and Basin-Scale Variation in Mixed Layer Depth and the Impact on Biological Production in the Central and North Pacific, 1960–1988', *Deep-Sea Res.* **42**, 1701–1716.

Sarmiento, J. L., Hughes, T. M. C., Stouffer, R. J., and Manabe, S.: 1998, 'Simulated Response of the Ocean Carbon Cycle to Anthropogenic Climate Warming', *Nature* **393**, 245–249.

Sarmiento, J. L., Slater, R. D., Fasham, M. J., Ducklow, H. W., Toggweiler, J. R., and Evans, G. T.: 1993, 'A Seasonal Three-Dimensional Ecosystem Model of Nitrogen Cycling in the North Atlantic Euphotic Zone', *Global Biogeochem. Cycles* **7**, 417–450.

Sarmiento, J. L. and Toggweiler, J. R.: 1984, 'A New Model for the Role of the Oceans in Determining Atmospheric pCO_2', *Nature* **308**, 621–624.

Shaffer, G.: 1993, 'Effects of the Marine Biota on Global Carbon Cycling', in Heimann, M. (ed.), *The Global Carbon Cycle*, Springer-Verlag, Berlin, pp. 431–455.

Smith, R. D., Dukowicz, J. K., and Malone, R. C.: 1992, 'Parallel Ocean General Circulation Modeling', *Physica D* **60**, 38–61.

Sverdrup, H. U.: 1953, 'On Conditions for the Vernal Blooming of Phytoplankton', *J. Cons. Int. Explor. Mer* **18**, 287–295.

Taylor, A. H., Geider, R. J., and Gilbert, F. J. H.: 1997, 'Seasonal and Latitudinal Dependencies of Phytoplankton Carbon-to-Chlorophyll a Ratios: Results of a Modelling Study', *Marine Ecology-Progress Series* **152**, 51–66.

Washington, W. M., Weatherly, J. W., Meehl, G. A., Semtner, A. J., Bettge, T. W., Craig, A. P., Strand, W. G., Arblaster, J., Wayland, V. B., James, R., and Zhang, Y.: 2000, 'Parallel Climate Model (PCM) Control and Transient Simulations', *Clim. Dyn.* **16**, 755–774.

Zhang, J. and Hibler, W. D.: 1997, 'On an Efficient Numerical Method for Modeling Sea Ice Dynamics', *J. Geophys. Res.* **102**, 8691–8702.

(Received 21 June 2002; in revised form 18 June 2003)